Int. J. Heat Mass Transfer. Vol. 27, No. 10, pp. 1873–1878, 1984
Printed in Great Britain

0017-9310/84 \$3.00 + 0.00
Pergamon Press Ltd.

Thermal boundary layer thickness in the cylinder of a spark-ignition engine

EDWARD J. LYFORD-PIKE
Cummins Brazil SA, São Paulo, Brazil

and

JOHN B. HEYWOOD
Sloan Automotive Laboratory, Massachusetts Institute of Technology, Cambridge, MA 02139, U.S.A.

(*Received* 28 *September* 1983 *and in revised form* 24 *January* 1984)

Abstract—The thicknesses of the thermal boundary layers in the cylinder of a spark-ignition engine were measured throughout the complete operating cycle. The engine used for these experiments was a special visualization engine with a square cross-section 'cylinder' and two quartz glass walls. Measurements of thickness were taken at different locations, speeds and loads, from schlieren photographs. The results show that the layers on the cylinder wall reach a maximum thickness of about 2 mm at the end of expansion. On the cylinder head and piston top, the layers are two to three times thicker. Reducing engine speed resulted in thicker layers, while changing load showed no significant effects on thickness. It is shown that on the cylinder wall, the thermal boundary layer thickness depends on thermal diffusivity and the time available for the layer to develop. The growth of this layer was correlated with an expression in the form $\delta_T \sqrt{(\alpha t)} \propto Re^{0.2}$.

BACKGROUND

THE BEHAVIOR of the thermal boundary layer during the operating cycle of a spark-ignition engine plays an important role in several engine processes. It governs engine heat transfer. It influences the quenching of the flame near the wall. The hydrocarbon emissions are known to originate in crevices, oil layers and deposits on or adjacent to the combustion chamber walls. The boundary layer characteristics will affect hydrocarbon formation in these regions, and post-formation mixing and oxidation processes. This paper presents the results of measurements of the thickness of the thermal boundary layer on different parts of the combustion chamber (the cylinder wall, the cylinder head and the piston) through the engine's operating cycle. For the layer on the cylinder wall, a simple unsteady boundary layer scaling law is shown to correlate the data.

TEST ENGINE AND PROCEDURES

The special spark-ignition engine used for the measurement of thermal boundary layer thickness is shown in Fig. 1. The engine was designed to permit visualization of the entire cylinder volume through the complete engine operating cycle [1]. This was accomplished by using a square cross-section 'cylinder' with two parallel optical quality quartz walls for windows, and a square cross-section piston. A schlieren optical system which fills the cylinder with a parallel beam of light was used to observe those flow features which are defined by density gradients.

The basis for this research engine was a removable head Cooperative Fuel Research (CFR) engine. As shown in Fig. 1, the visualization engine uses the crankcase and internal parts of the CFR engine as its lower half. The CFR engine was split between the cylinder and head. The new portion of the visualization engine is the square cross-section assembly. The new square cross-section piston was connected to the CFR piston via a rigid rod; the CFR piston and cylinder acted, therefore, as a type of crosshead. The original

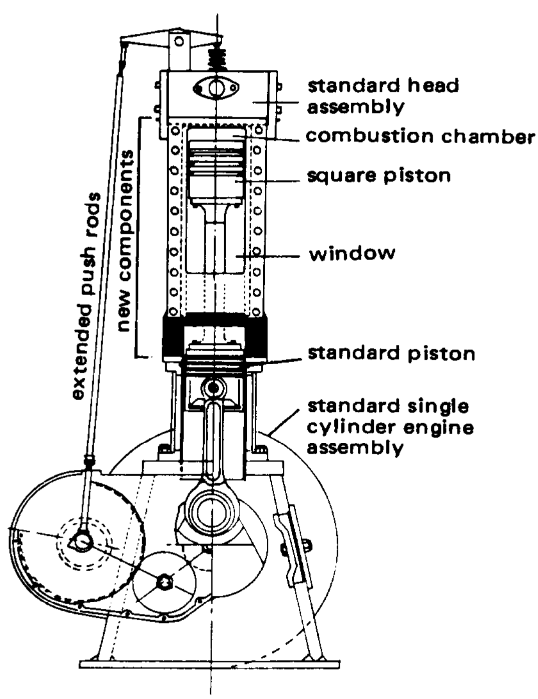

FIG. 1. Square cross-section flow visualization engine.

NOMENCLATURE

c_p	specific heat at constant pressure
I	illumination
ΔI	change in illumination
k	gas thermal conductivity
p	gas pressure
Re	Reynolds number
T	gas temperature
t	time
v	gas velocity
v_p	piston velocity
x	distance of top of piston from cylinder head
x_0	distance of measurement location from cylinder head
y	distance from wall.

Greek symbols

α	thermal diffusivity
δ_T	thermal boundary layer thickness
μ	gas viscosity
ρ	gas density.

CFR engine cylinder-head, valves and valve mechanism were used on top of the new square cross-section assembly. Three sets of hard graphite 'rings', which overlapped at the corners, provided the gas seal; they operated without lubrication. Geometric details of the square cross-section transparent cylinder assembly are given in Table 1. The fuel, propane, was mixed with the airflow in a tank to ensure mixture uniformity. The tank also damped out intake flow pulses. The tank was connected to the engine through a throttle valve.

The schlieren set-up used was the Z-type layout [2]. The source aperture was circular and its diameter was held constant at 1.6 mm. The cut-off aperture was also circular, and its diameter was varied about the same value. The schlieren system, therefore, responded to density gradients in any direction. Two types of photographs were taken. Still pictures were taken with a microflash unit, triggered at a preset crank angle. Movies were taken at 2000 frames per second with a 1/10 shutter speed to control the exposure of each frame.

The operating procedure for each experimental run was as follows. The engine was motored at preset conditions. The fuel was then turned on for at least 15 s to ensure a homogeneous mixture in the fuel–air mixing tank. For still photographs, the ignition system was then switched on and the engine permitted to fire for about 10 cycles. The pressure data for the particular cycle to be photographed was then recorded. For schlieren movies, the same procedure was followed. After the ignition system was switched on, about 16 cycles were filmed and their pressure data recorded.

The engine operating conditions used in this study are given in Table 2. A previous study [1] has shown that the operating characteristics of this visualization engine are sufficiently close to those of real engines for the results to provide useful insights. For example, at half-throttle, the standard deviation in peak cylinder pressure is 1 atm which is about 10% of the mean peak pressure of 9.7 atm. This is comparable to the part-load behavior of normal engines.

EXAMPLES OF PHOTOGRAPHS

Figure 2 shows typical still photographs taken during different parts of the engine cycle. Figure 2(a) shows the start of the intake process; the front of the jet-like flow through the valve, as it moves towards the cylinder wall, is evident. Figure 2(b) shows the flame when its front has moved about 80% of the way from the spark plug in the upper right-hand corner to the far wall. At this point about one-quarter of the charge has burned [1]. Figure 2(c) shows the cylinder about halfway through the expansion process. The edge of the thermal boundary layer—the dark irregular edge which surrounds the combustion chamber—is clearly visible in all these photographs. In Fig. 2(c), the picture

Table 1. Geometric details of transparent engine

Bore (square), mm	82.6
Stroke, mm	114.3
Compression ratio	4.8
Connecting rod length, mm	254
Intake valve:	
diameter, mm	31.5
maximum lift, mm	5.7
opens at	10° ATC
closes at	34° ABC
Exhaust valve:	
diameter, mm	31.5
maximum lift, mm	6.0
opens at	140° ATC
closes at	15° ATC

Table 2. Engine operating conditions

Engine speed	1380 rpm, 815 rpm
Inlet pressure	0.5 atm, 0.7 atm
Inlet temperature	25°C
Exhaust pressure	1 atm
Equivalence ratio (fuel/air)	1.15
Spark-timing set for max. brake torque:	
at 1380 rpm, 0.7 atm	42° BTC
at 1380 rpm, 0.5 atm	55° BTC
at 815 rpm, 0.7 atm	65° BTC

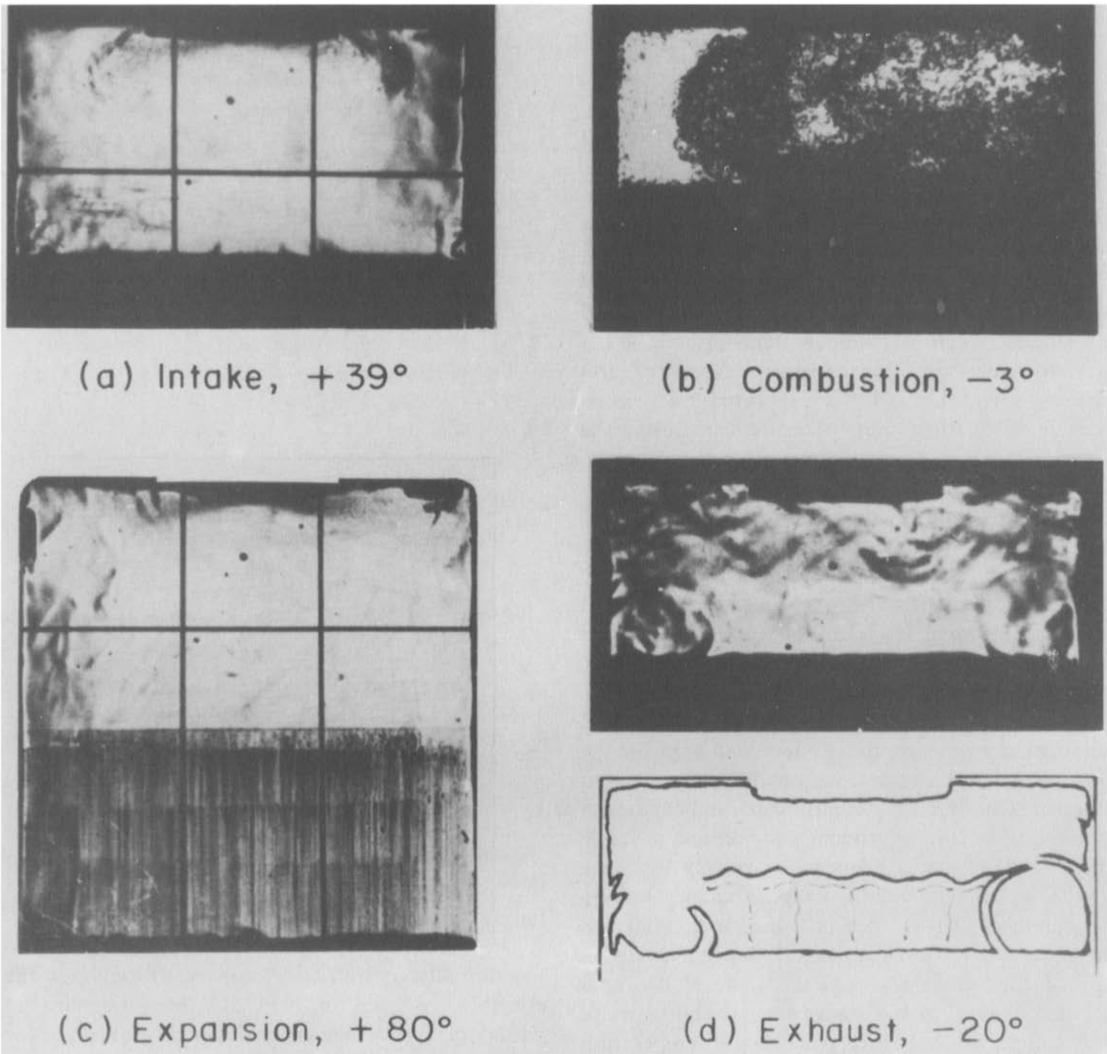

FIG. 2. Schlieren photographs of engine cylinder at different times during the engine operating cycle. Crank angles are relative to top center. (a) Shows start of the intake flow into the cylinder. (b) Shows flame during combustion. (c) Shows thermal boundary layer thicknesses on the chamber walls during expansion. (d) Shows vortex flow in the piston cylinder wall corner set up during the exhaust stroke.

has been cut out along the actual combustion chamber wall location to indicate the thickness of the thermal boundary layer around the chamber. The boundary layer is thicker on the piston crown and on the cylinder head than on the cylinder walls. On the cylinder wall, the boundary layer decreases in thickness from the piston crown position at top center to the actual piston crown position. [The plug in the upper left-hand corner of Fig. 2(c) was used for other analysis. The streaked region in the lower half of Fig. 2(c) results from carbon from the piston rings. The horizontal and vertical wires are outside the cylinder and were used as a reference for geometrical measurements.]

Figure 2(d) shows the cylinder towards the end of the exhaust stroke. A vortex flow pattern in the piston/cylinder wall corner (identified in the schematic) is set up as the piston scrapes off and rolls up the boundary layer on the cylinder wall [3]. The substantial irregularity in boundary layer thickness at this point in the cycle is evident.

THERMAL BOUNDARY LAYER THICKNESS

The schlieren system was set up to be sufficiently sensitive to give complete extinction of light deflected from the beam close to the outer edge of the boundary layer. The schlieren technique responds to density gradients in the flow field. For uniform pressure, p, the fractional change in illumination, $\Delta I/I$, can be expressed in terms of the temperature and temperature gradient [2]

$$\frac{1}{T^2}\frac{\mathrm{d}T}{\mathrm{d}y} = \frac{\text{const.}}{p}\frac{\Delta I}{I}.$$

In these experiments, the value of $(1/T^2)(\mathrm{d}T/\mathrm{d}y)$ needed for complete extinction given by this equation was always much smaller than values estimated for the thermal boundary layer assuming a linear profile between the wall and bulk gas temperature.

Measurements of boundary layer thickness were made from photographs and movies. The vertical and horizontal wires visible in Figs. 2(a) and (c) served as the geometric reference. Measurements from the still pictures were taken with a calibrated microscope accurate to ± 0.025 mm. Measurements from the movies were taken directly from a projected image 2.5 times larger than the engine, and the error was estimated to be of the order of ± 0.05 mm. Measurements of the layer thickness for ten consecutive cycles at one location on the cylinder wall halfway through the expansion stroke showed a standard deviation of 0.1 mm, equivalent to 5% of the thickness at that location. During the exhaust and intake processes, cycle-by-cycle variations were larger, however.

Figure 3 shows the thermal boundary layer thickness measured at a point on the cylinder wall opposite the spark plug. The thickness decreases during intake, and increases steadily during compression and expansion to about 2 mm. It stops growing and becomes unstable when the exhaust valve opens, separating from the cylinder wall and interacting with the bulk gas leaving the chamber. The absence of a measured thickness during most of the intake process is due to a change in sign of the temperature gradient when the cool incoming charge [see Fig. 2(a)] reaches the hotter walls. Only the points that correspond to gas temperature higher than wall temperature are plotted. The wall temperature was estimated to be about 400 K. During

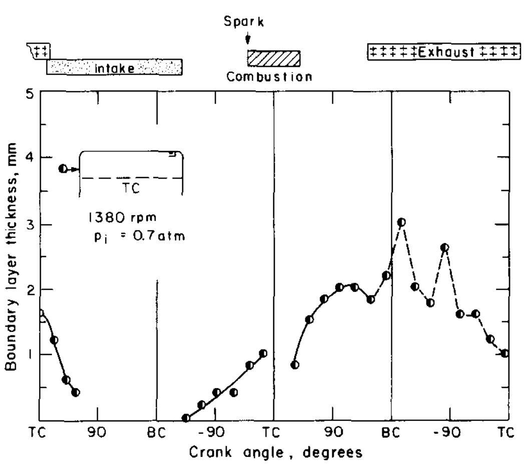

FIG. 3. Thickness of the thermal boundary layer on the cylinder wall in the clearance volume, through the complete engine operating cycle.

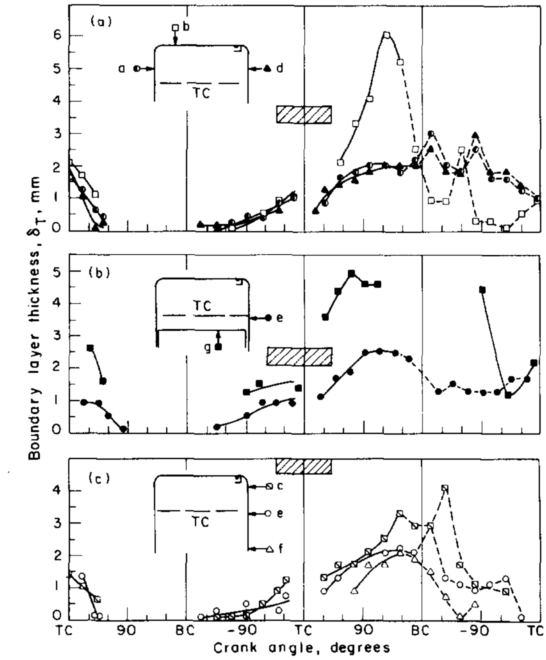

FIG. 4. Thickness of the thermal boundary layer at locations on the cylinder wall, cylinder head and piston through the engine operating cycle. Cross-hatched bars show the duration of the combustion process.

combustion, our view of the layer is interrupted from the time the flame arrives until the inflamed charge on the wall is completely burned [see Fig. 2(b)].

The thickness of the thermal boundary layers varies substantially at different locations throughout the chamber, as seen in Fig. 2(c). Measurements of boundary layer thickness were made at locations on the cylinder head, piston and cylinder wall throughout the engine cycle to define this variation. Figure 4 shows the results. During the intake and compression processes all the results show similar trends [though the layer on the piston crown is thicker, see Fig. 4(b)]. After combustion, the layers on the cylinder head [Fig. 4(a)] and piston crown [Fig. 4(b)] grow much faster than the layers on the cylinder wall. When the exhaust valve opens, the boundary layer thickness decreases rapidly during blowdown [the period before bottom center (BC) when the cylinder pressure drops rapidly to the exhaust pressure level], and the boundary layer becomes unstable at all three locations. Figure 4(c) shows the variation in boundary layer thickness at different locations on the cylinder wall. While location (c) is in the clearance volume, locations (e) and (f) are covered by the piston during portions of the cycle, and layers at these two points cannot develop until they are uncovered by the moving piston. The layer at (c) is the thickest; during expansion, the layers at (e) and (f) commence growing at successively later times.

The thicknesses of the layers on the cylinder head and piston top are two to three times thicker than for points along the walls. We speculate that this is due to the different velocity fields in those regions: the piston-induced gas motion is along the cylinder axis, parallel to the cylinder walls and perpendicular to the cylinder head and piston crown.

Measurements were also taken at reduced speeds and loads. A reduction of speed from 1380 to 815 rpm shows a 20–30% increase in layer thickness during expansion. The growth of the layer is time dependent and at lower engine speeds the layer has a longer time period to develop. Reducing the load to 0.5 atm from 0.7 atm showed no significant effect in the thickness of the layer and its development.

Estimates of thermal boundary layer thickness in spark-ignition engines, based on empirical heat transfer correlations and thermal energy conservation for the growing layer, give similar results [4, 5]. For close to the same engine operating conditions, the thermal boundary layer was predicted to grow during expansion to about 3 mm thick at 90° after top center (ATC). Note that a substantial fraction of the cylinder mass is contained in the thermal boundary layer. For example, for an average layer thickness of 3 mm at 90° ATC during expansion, the volume of the boundary layer for typical engine dimensions is 20% of the combustion chamber volume. Since the average density in the boundary layer is about twice that in the bulk gases, some 30–40% of the cylinder mass is contained within the boundary layer.

CORRELATION OF CYLINDER WALL RESULTS

Dimensional analysis was used to develop a correlation for the growth of the thermal boundary layer on the cylinder wall during the expansion process. The following quantities were taken as the relevant parameters determining the thermal boundary layer thickness, δ_T: gas thermal conductivity, k; density, ρ; specific heat at constant pressure, c_p; viscosity, μ; and time, t. All gas properties were evaluated at the mean of the bulk gas temperature and the wall temperature.

The local gas velocity v was evaluated by assuming a one-dimensional axial gas flow with velocity varying linearly from zero at the cylinder head to the piston velocity v_p at the piston crown: i.e.

$$v = v_p(x_0/x)$$

where x is the distance between the piston crown and the cylinder head; v is not defined for $x < x_0$.

The gas properties were evaluated using the correlations and data in ref. [6]. The elapsed time t for locations below the TC piston position begins at the moment they are uncovered by the piston. Since there is uncertainty about the starting time for locations above piston top-center position, this top-center position is defined as the starting time for all locations in the clearance volume.

Since $\delta_T/(\alpha t)^{1/2} \approx 3$, where $\alpha = k/(\rho c_p)$, the development of the layer in this engine is a Rayleigh-type

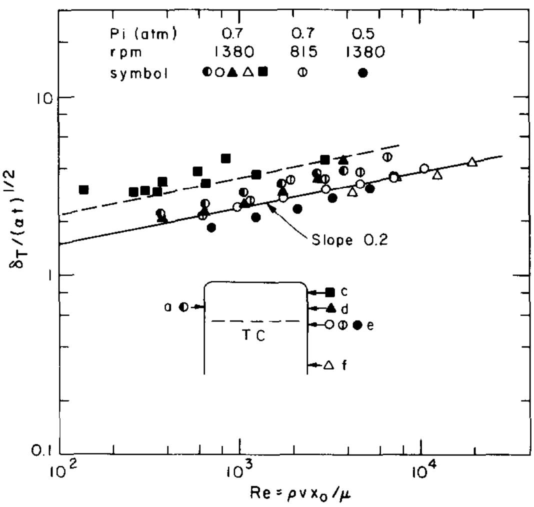

FIG. 5. Correlation of dimensionless boundary layer thickness on the cylinder wall against Reynolds number based on local gas velocity.

problem. Figure 5 shows that most of the data are fitted by the correlation

$$\delta_T/(\alpha t)^{1/2} = 0.6 Re^{0.2}$$

where the Reynolds number $Re = \rho v x_0/\mu$, which is shown as the solid line. The data for location (c), close to the cylinder head, lie above the correlation, however. It was observed from the schlieren movies that at locations less than two-thirds the clearance height from the cylinder head, the piston speed proportionality law did not apply for the gas velocity; measured velocities were substantially higher. A Reynolds number calculated using the gas velocity measured directly from the movies results in the dotted line which now correlates this data adequately.

Acknowledgement—This work was supported in part by a grant from General Motors Research Laboratories and a grant from the Ford Motor Company.

REFERENCES

1. M. Namazian, S. Hansen, E. Lyford-Pike, J. Sanchez-Barsse, J. Heywood and J. Rife, Schlieren visualization of the flow and density fields in the cylinder of a spark-ignition engine, Paper 800044, *S.A.E. Trans.* **89**, 276–303 (1980).
2. L. A. Vasil'ev, Schlieren methods, Israel Program for Scientific Translation Ltd. (1971).
3. R. J. Tabaczynski, D. P. Hoult and J. C. Keck, High Reynolds number flow in a moving corner, *J. Fluid Mech.* **42**, 249–255 (1970).
4. J. B. Heywood, J. M. Higgins, P. A. Watts and R. J. Tabaczynski, Development and use of a cycle simulation to predict SI engine efficiency and NO_x emissions, SAE paper 790291 (1979).
5. G. A. Lavoie and P. N. Blumberg, A fundamental model for predicting fuel consumption, NO_x and HC emissions of the conventional spark-ignited engine, *Combust. Sci. Technol.* **21**, 225–258 (1980).
6. S. H. Mansouri and J. B. Heywood, Correlations for the viscosity and Prandtl number of hydrocarbon–air combustion products, *Combust. Sci. Technol.* **23**, 251–256 (1980).

EPAISSEUR DE COUCHE LIMITE THERMIQUE DANS UN CYLINDRE AVEC BOUGIE DE MOTEUR A EXPLOSION

Résumé—Les épaisseurs des couches limites thermiques dans le cylindre d'un moteur à explosion sont mesurées pendant le cycle complet. Le moteur utilisé permet une visualisation avec un cylindre à section droite carrée et deux parois à quartz. Des mesures sont effectuées en différents endroits, à différentes vitesses et charges par des photographies rapides. Les résultats montrent que les couches sur la paroi du cylindre atteignent une épaisseur maximale d'environ 2 mm à la fin de la détente. Sur la tête du cylindre et le sommet du piston, les couches sont deux à trois fois plus épaisses. Une réduction de vitesse s'accompagne d'un épaississement, tandis qu'un changement de charge ne montre pas d'effet sur l'épaisseur. On montre que sur la paroi du cylindre, l'épaisseur de couche limite thermique dépend de la diffusivité thermique et du temps offert à la couche pour son développement. La croissance de cette couche est exprimée par une expression de la forme $\delta_T/\sqrt{(\alpha t)} \propto Re^{0,2}$.

DICKE DER THERMISCHEN GRENZSCHICHT IM ZYLINDER EINES OTTO-MOTORS

Zusammenfassung—Die Dicke der thermischen Grenzschicht im Zylinder eines Otto-Motors wurde während des vollständigen Arbeitszyklusses gemessen. Die Maschine, die für diese Versuche verwendet wurde, war besonders zur Sichtbarmachung der Vorgänge geeignet. Sie hatte einen Zylinder von quadratischem Querschnitt und zwei Quarzglaswände. Dickemessungen wurden an verschiedenen Stellen bei unterschiedlichen Geschwindigkeiten und Belastungen mit Hilfe von Schlieren-Fotografien gemacht. Die Ergebnisse zeigen, daß die Grenzschicht an der Zylinderwand am Ende der Expansion eine maximale Dicke von 2 mm erreicht. Am Zylinderkopf und am Kolbenboden war die Grenzschicht zwei bis dreimal so dick. Eine Verringerung der Geschwindigkeit führt zu einer dickeren Grenzschicht, während eine Änderung der Last keinen nennenswerten Einfluß auf die Dicke hat. Es zeigte sich, daß die Dicke der thermischen Grenzschicht an der Zylinderwand von der Temperaturleitfähigkeit und der Zeit, die zur Ausbildung der Grenzschicht zur Verfügung steht, abhängt.

ТОЛЩИНА ТЕПЛОВОГО ПОГРАНИЧНОГО СЛОЯ В ЦИЛИНДРЕ ДВИГАТЕЛЯ С ИСКРОВЫМ ЗАЖИГАНИЕМ

Аннотация—Проводилось измерение толщины теплового пограничного слоя в цилиндре двигателя с искровым зажиганием в течение всего рабочего цикла. Исследования выполнялись на специальной визуалиационной модели двигателя с «цилиндром» квадратного сечения и двумя стенками из кварцевого стекла. Измерения толщины проводились теневым методом в разных местах цилиндра, при различных числе оборотов и нагрузке. Результаты показывают, что максимальная толщина слоев на стенке порядка 2 мм имеет место в конце цикла расширения. На головке цилиндра и в верхней части поршня толщина слоев в 2–3 раза больше. При меньшем числе оборотов двигателя толщина слоев больше, в то время как изменение нагрузки не оказывает существенного влияния на толщину. Показано, что толщина теплового пограничного слоя на стенке цилиндра зависит от температуропроводности и времени, в течение которого развивается слой. Рост толщины слоя описывается зависимостью типа $\delta_T\sqrt{(\alpha t)} \propto Re^{0,2}$.